



Improvement of water filtration performance of graphene oxide membranes on Nylon support by UV-assisted reduction treatment: Control of molecular weight cut-off

M. Fernández-Márquez, R. Pla, A.S. Oliveira, J.A. Baeza, L. Calvo, N. Alonso-Morales^{*}, M.A. Gilarranz

Department of Chemical Engineering, Universidad Autónoma de Madrid, 28049 Madrid, Spain

ARTICLE INFO

Keywords:

Graphene oxide
Membrane
Rejection
UV-assisted reduction treatment

ABSTRACT

Graphene oxide (GO) membranes on Nylon support were modified by UV-assisted reduction to control their behavior in the filtration of water containing organic pollutants. Pyridine, phenol, 2-naphthol and disperse blue 3 were used as probe pollutants to determine the molecular weight cut-off (MWCO) of the membranes prepared. The membranes were prepared with GO loads of 0.04 and 0.06 mg cm⁻² and subjected to UV radiation from a Hg lamp (30 W m⁻²) for 30–60 min. The non-irradiated membranes showed MWCO ca. 300 Da, with rejection values above 90 % for disperse blue 3, while rejection for 2-naphthol reached 64 %. Irradiation resulted in substantial removal of oxygen surface groups, leading to staking of GO sheets and a decrease of interlayer space. These structural changes narrowed the size of pores thus reducing solutes passage. Rejection of 2-naphthol reached 83 %, i.e. decreasing MWCO to ca. 150 Da. The increase in the rejection of solutes was higher for membranes with a GO load of 0.06 mg cm⁻², however similar water permeability was achieved regardless the GO load. UV-reduction shows a high potential for controlling the rejection of solutes by GO membranes on Nylon support while maintaining good permeability.

1. Introduction

In the last few decades, freshwater availability has decreased. Water scarcity is expected to increase even more in the following years due to population growth and climate change [1,2]. In this scenario, effective water treatment systems become vital to manage wastewater and ensure a clean water supply from polluted and alternative sources.

The technologies available for water treatment include physical, chemical, and biological methods [3]. Biological methods are the most widespread for wastewater treatment. Combination with physical and chemical methods is usually needed for final adjustment of water quality, including removal of pathogens and micropollutants. Physical and chemical methods are also the main options for the treatment of raw water for drinking water production. However, traditional treatment techniques show a limited removal efficiency for some pollutants, like dyes or emerging contaminants. Thus, in primary treatments, typically sedimentation and flotation, less than 10% of removal is achieved for contaminants like pesticides or pharmaceuticals [4]. Secondary

treatment, which is a combination of biological and physical methods, shows higher removal efficiency. Despite that, complete mineralization is not usually achieved for some compounds, leading to the presence of harmful byproducts. In addition, the toxicity of some pollutants can inhibit the biodegradation process [5]. For that reason, tertiary treatment is usually needed to ensure complete removal of contaminants.

Since traditional technologies show limitations, a variety of chemical and physical methods have been proposed as alternatives for water treatment. Among chemical methods, advanced oxidation processes have been the most studied [6]. Some of these technologies present economic issues due to large energy consumption. On the other hand, physical methods present some advantages over chemical technologies, since they are more simple, easily scalable and flexible, among others [3].

Physical methods include technologies such as advanced flocculation, sand filtration, membrane filtration or adsorption. Membrane filtration has been widely studied in the last years. It stands out for flexibility, allowing for separation of pollutants from water by sieving,

^{*} Corresponding author.

E-mail address: noelia.alonso@uam.es (N. Alonso-Morales).

<https://doi.org/10.1016/j.cej.2022.137807>

Received 25 March 2022; Received in revised form 24 June 2022; Accepted 25 June 2022

Available online 27 June 2022

1385-8947/© 2022 The Authors. Published by Elsevier B.V. This is an open access article under the CC BY-NC license (<http://creativecommons.org/licenses/by-nc/4.0/>).

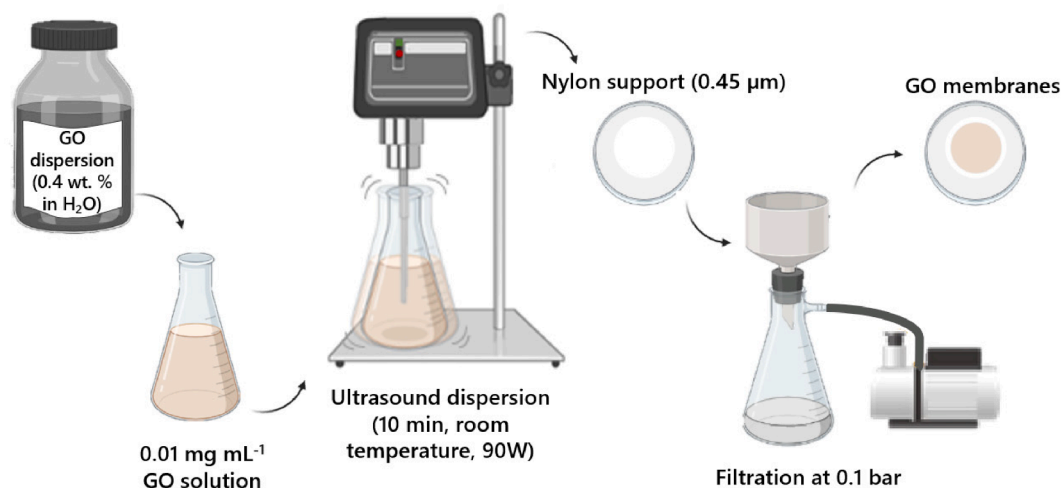


Fig. 1. Schematic illustration of GO membranes on Nylon support preparation process.

size exclusion or adsorption, among other mechanisms, depending on the properties of the compounds [7]. This method offers some advantages such as small and scalable equipment, low energy requirements, or the possibility of working without chemicals consumption [8].

Polymeric membranes have been used traditionally as filtration media, but carbon-based materials have emerged as candidates for the construction of membranes for water treatment. Among them, graphene and its derivatives, especially graphene oxide (GO), are promising due to their tuneable structure and their mechanical, thermal, and electrical properties. Self-supporting membranes fabricated only with GO or rGO require high thickness for achieving sufficient mechanical strength. Therefore, GO membranes are usually supported to improve high-pressure resistance and to reduce the thickness of the GO filtration layer for better filtration performance [9].

GO membranes can be formed by different methods including coating, layer-by-layer, or pressure-assisted. The pressure-assisted method is one of the most interesting ones because it allows for facile tuning of membrane properties. In this method, a GO suspension is prepared and filtered through a support, resulting in stacked GO layers retained over the support. Membrane thickness can be adjusted by modifying the volume or concentration of GO precursor solution. Other variables such as deposition rate can be controlled to improve membrane performance [10].

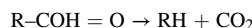
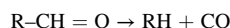
GO membranes have great versatility since they are suitable for a wide variety of applications. These membranes have demonstrated remarkable performance in dye filtration. Some researchers have achieved dyes removal rates greater than 95 % using GO membranes [11]. Poly- and perfluoroalkyl substances (PFAS) represent another interesting family of pollutants tested in filtration with GO-based membranes, showing retentions over 90 % [12]. GO membranes have also been tested in water desalination, achieving relevant rejections for salts such as Na_2SO_4 [13].

Improved performance of GO membranes can be achieved through customization of starting GO nanosheets and GO membranes structure. Physical modifications include modification of GO nanosheets size and membrane thickness, or intercalation of additional materials for better control of pore size and hence filtration performance [9,14–16]. Chemical modifications can be achieved by functionalization with compounds such as amines [9]. Amine treatment leads to longer interlayer spacings since they intercalate between GO layers [17]. Chemical reduction of GO membranes leads to a smaller interlayer spacing, due to removal of surface oxygen groups, which enhances salts and organic compounds rejection, but also affects hydrophilicity and modifies water transport [18]. Chemical reduction with L (+)-ascorbic acid was tested successfully in membranes for dye filtration [19]. Hydrothermal

reduction has also been proven as a suitable option in salt rejection studies [18].

Photoreduction has been studied as an interesting alternative to achieve reduction of functional groups with high efficiency, low cost and improved reduction degree control with some selectivity in the reduction of specific surface groups, among other advantages [20,21]. Reduction can be achieved by direct irradiation without the aid of photocatalysts, which is of great interest for scalability application in industrial practice [22]. UV reduction has been tested successfully in membranes for improved dye filtration [23].

The modification of oxygen groups by UV radiation involves bond dissociation and photoinduced migration of epoxy and hydroxyl groups to the GO nanosheets edge, and the subsequent dissociation of these terminal groups under UV radiation. The reduction of hydroxyl group in the GO structure can be accompanied by the simultaneous elimination of hydrogen. Likewise, the reduction of carbonyl and carboxyl groups leads to the formation of CO and CO_2 , according to the general reactions [24,25]:



The current work explores the modification of GO membranes on Nylon support by UV radiation to improve filtration performance and control of molecular weight cut-off (MWCO). A commercial support has been selected to increase mechanical strength and reduce the thickness needed for the GO layer, and to facilitate scaling up of the results to larger surface membranes. The influence of GO layer thickness and UV irradiation time is studied to control rejection of solutes and increase permeability. Water solutions of organic compounds different molecular size are filtered through the modified membranes to evaluate behaviour and determine MWCO. The results obtained are representative of the applicability of the membranes in the treatment of drinking and reclaimed water.

2. Experimental

2.1. Materials

Graphene oxide (GO) dispersion (0.4 wt% in H_2O) was purchased from Graphenea® (Spain). Pyridine (greater than 99 %), phenol (99 %), 2-naphthol (99 %) and disperse blue 3 (Dye content 20 %) were purchased from Sigma-Aldrich. The Nylon supports employed in this work were supplied by Filtros Anioia (MNY045047N, Spain). They are made of polyamide 66 fibers. The supports have pore size of 0.45 μm and a

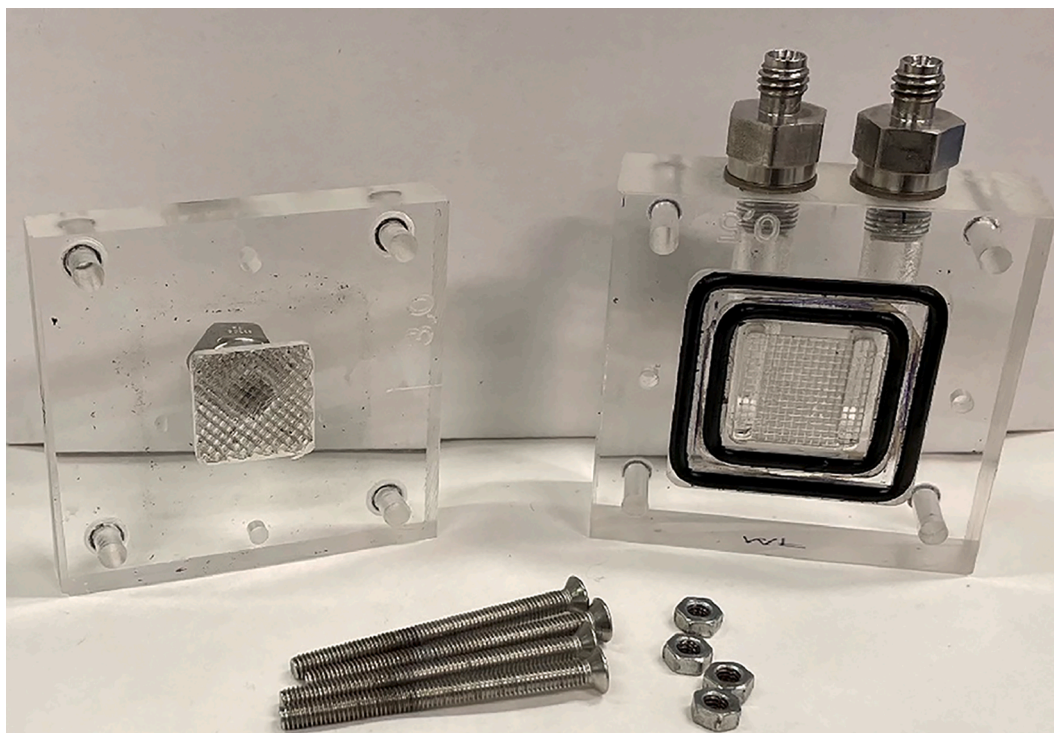


Fig. 2. Cross-flow device used in the permeation experiments.

thickness of 0.100–0.120 mm. The support has a flow rate for deionized water of $27 \text{ mL min}^{-1} \text{ cm}^{-2}$ (70 kPa).

2.2. Preparation of GO membrane on Nylon support

The GO membranes on Nylon support (GOM) were prepared by pressure-assisted filtration as described elsewhere [26,27]. Concentrated commercial GO dispersion was diluted to 0.01 mg mL^{-1} for the preparation of membranes. The solution was dispersed by sonication at room temperature during 10 min by applying an ultrasonic power of 90 W. The dispersed GO solution was filtered at 0.1 bar through a Nylon support. The schematic illustration of the process for the preparation of GO membranes on Nylon support is shown in Fig. 1.

The membranes were prepared with two different GO loads by filtering 40 or 60 mL of GO solution, equivalent to 0.04 and 0.06 mg cm^{-2} of GO in the membrane, and were denoted as GOM-0.04 and GOM-0.06, respectively. The range for GO load was selected according to previous screening tests, where it was found that filtration time for the preparation of membranes with a GO load of 0.08 mg cm^{-2} was very long (6.2 h), due to the higher volume of GO suspension needed, whereas for the 0.04 and 0.06 mg cm^{-2} membrane, filtration time was 1.0 and 1.5 h, respectively. The longer filtration time also led to higher compaction of the GO layer of the membrane, which combined to higher thickness resulted in too low permeability. After filtration, the prepared membranes were dried in an oven at 60°C during 24 h and stored at 12°C for 4 days before testing.

2.3. Preparation of rGO membranes on Nylon support

The reduced GO membranes on Nylon support (rGOM) were obtained by reduction of GOM by a UV lamp radiation [28]. To assess the effect of the reduction degree of the membranes, they were reduced during a 30 and 60 min. The reduction treatment was performed with a 150 W medium pressure Hg lamp (TQ-150 from Heraeus) contained in a water-cooled quartz chamber provided with a temperature control unit Ministat 125 (Huber). The lamp was enclosed in a security cabinet to

avoid hazardous UV irradiation spread. The lamp emits in a broad spectrum between 250 and 600 nm, with a UV-irradiance of 30 W m^{-2} .

2.4. Characterization of GO and rGO membranes on Nylon support

The morphology of GOM and rGOM surface was characterized by scanning electron microscopy (SEM, FEI Verios 460 Field Emission Microscope). The distribution of functional groups in the membranes was analysed by FTIR spectroscopy (Perkin Elmer Spectrum Two), that was performed in Attenuated Total Reflectance (ATR) mode in the wave-number range of $450\text{--}4000 \text{ cm}^{-1}$, with no need of preparation of the sample, by pressing the sample area of interest against a diamond ATR specific crystal; and by X-ray photoelectron spectroscopy (XPS, K-Alpha Thermo Scientific equipped with an AlK α X-ray excitation source, 1486.68 eV). X-ray diffractometer (XRD, X-pert PRO Theta/2Theta, Panalytical) was used to measure the interlayer spacing of the GO layer of the membranes, which was calculated using the Bragg's law (Eq. (1)) [29]:

$$2d\sin\theta = \lambda \quad (1)$$

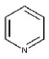
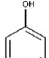
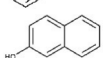
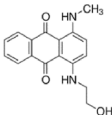
where d is the lattice spacing, θ is the diffraction angle and λ is the wavelength.

2.5. Filtration performance experiments

The filtration performance of the prepared GOM and rGOM was studied using the self-assembled cross-flow device shown in Fig. 2. Cross-flow cells are commonly used in filtration performance assessment due to similarities to commercial filtration modules [30]. The effective area of the membranes was 4 cm^2 . Permeability and rejection were evaluated at 2 bar and room temperature using a feed flow of 2 mL min^{-1} . Water filtration tests were carried out with water solutions of four model organic compounds (pyridine, phenol, 2-naphthol and disperse blue 3) with an initial concentration of 120 mg L^{-1} . The solutes were used as probe molecules thanks to their different molecular weight to determine the molecular weight cut-off (MWCO) of the membranes.

Table 1

Molecular structure, molecular size and molecular weight for the organic compounds used in the filtration experiments.

Compound	Molecular structure	Molecular size (Å)	Molecular weight (g mol ⁻¹)
Pyridine		4.9 × 3.9	79.1
Phenol		5.0 × 5.7	94.1
2-Naphthol		7.8 × 5.6	144.2
Disperse blue 3		11.1 × 11.3	296.3

MWCO here refers to the lowest solute molecular weight (in Da) that is 90% retained by a membrane. Table 1 shows the molecular structure, molecular size and molecular weight for all organic compounds used in the filtration experiments. The molecular size of the compounds was estimated using TURBOMOLE software. The feed solution and permeate concentration was measured by UV–VIS spectroscopy (Cary 60 UV–VIS spectrophotometer, Agilent). Before the filtration tests, the cross-flow system was fed with deionized water for 30 min, then the feed was switched to organic compound solution and samples were taken after stabilization for additional 30 min. In some selected experiments the membranes were kept in operation for at least 48 h, maintaining stable permeation and rejection values.

To evaluate the performance of the membranes in the filtration experiments, the permeance (L m⁻² h⁻¹ bar⁻¹) and rejection (%) were calculated from the following equations [21]:

$$\text{Permeance} = \frac{V}{t \times A \times P} \quad (2)$$

$$\text{Rejection} = \frac{C_i - C_p}{C_i} \times 100 \quad (3)$$

where V is the volume of permeate (L), t is the filtration time (h), A is the effective area of the membrane (m²), P is the transmembrane pressure (bar), and C_i and C_p are the feed concentration and the permeate concentration, respectively.

3. Results and discussion

3.1. Characterization of GOM and rGOM

Fig. 3 shows images of GOM-0.04 (a) and rGOM-0.04 after UV-assisted reduction for 30 (b) and 60 min (c). A significant change in

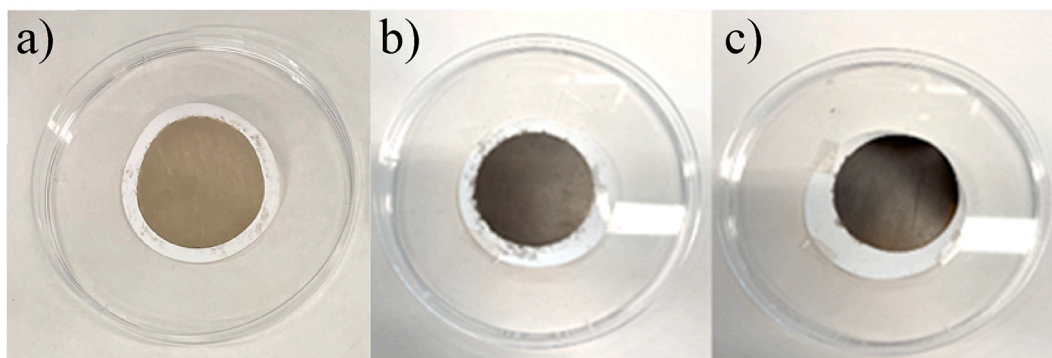


Fig. 3. Digital photos of GOM-0.04 (a), rGOM-0.04 after 30 min (b) and 60 min (c) UV-assisted reduction.

the color of the GO membranes on Nylon support can be observed after the reduction treatment. rGOM were darker than GOM (golden colour), revealing reduction and changes in the surface groups of the GO membranes on Nylon support due to the UV-assisted reduction treatment [31]. No significant differences were observed between the membranes prepared with GO loads of 0.04 and 0.06 mg cm⁻² (not shown).

Regarding FTIR-ATR analysis Fig. 4, the main peaks of Nylon support are at 3295 cm⁻¹, attributed to the N–H stretch from amino groups, at 2930 cm⁻¹, associated with a C–H stretching vibration due to alkanes group, and a series of strong peaks between 1500 and 1700 cm⁻¹ due to amide bands. The most evident at 1640 cm⁻¹ is related stretching of C=O from the carbonyl group of the amide, and the one at 1535 cm⁻¹ is due to C–N stretching and N–H bonding [32]. The peaks attributable to GO layer are around 1720 cm⁻¹ and 1080 cm⁻¹, assigned to C=O stretching of the COOH groups [33]. The UV treatment led to a reduction in carboxyl groups content at GO nanosheets, according with XPS analysis (see below), although only a slight decrease in the FTIR peak at 1375 and 1720 cm⁻¹ could be observed. The broad absorption from 3500 to 3700 cm⁻¹ and around 1625 cm⁻¹ was caused by the O–H stretching vibration of the surface hydroxyl groups on GO nanosheets [33], but again small differences were observed, due to the small amount of GO deposited on the Nylon support. The stretching of C=C bond is normally referred at around 1600 cm⁻¹ [34], although in the GO membranes on Nylon support this peak overlaps with the C=O band of the amine group.

XPS analysis was used to assess changes in the distribution functional

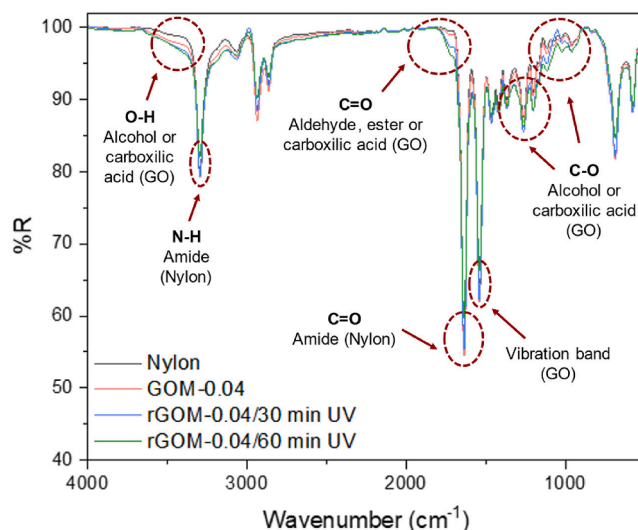


Fig. 4. FTIR analysis of nylon support, GO membrane on nylon support as prepared and reduced by UV treatment during 10, 30 and 60 min.

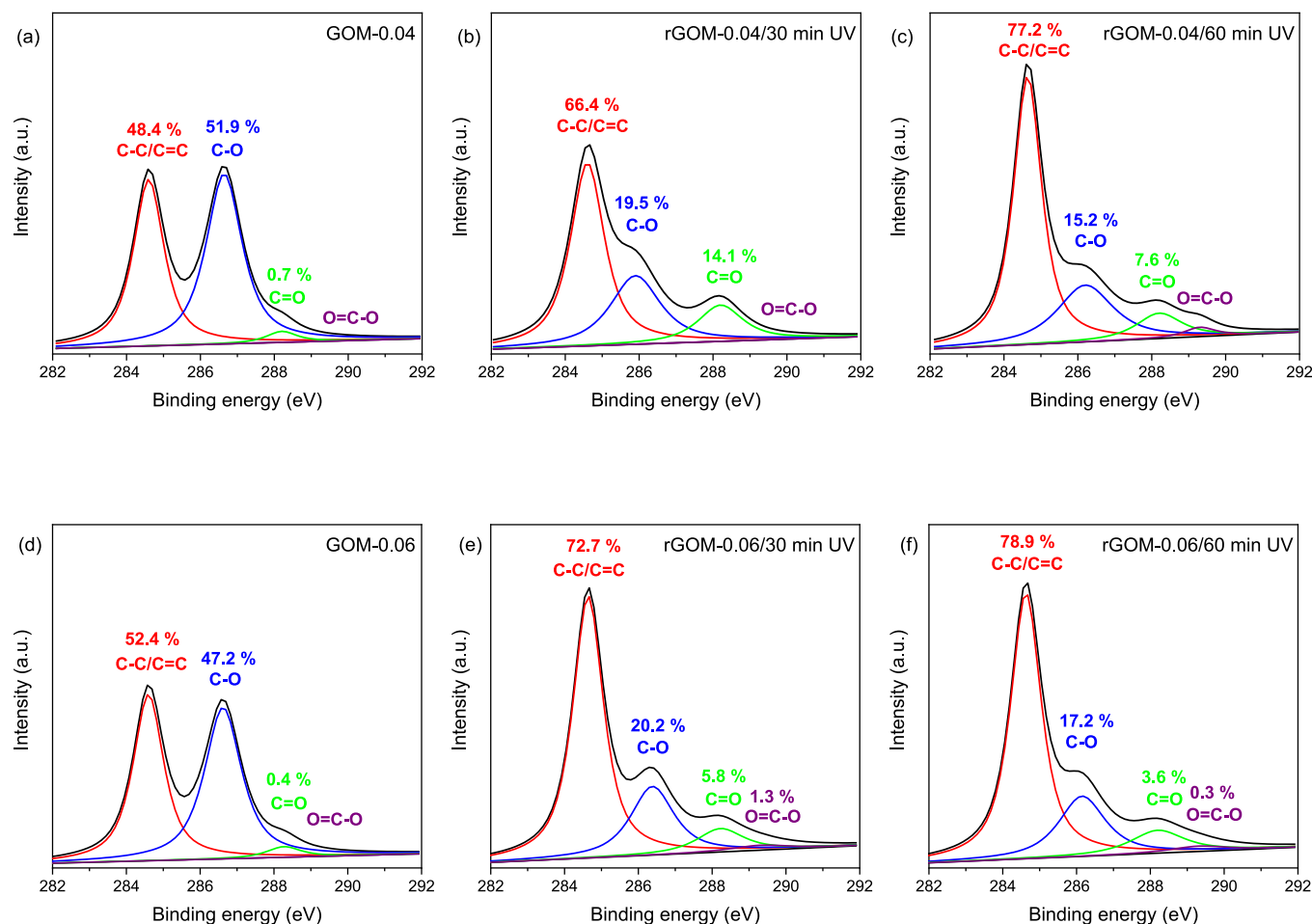


Fig. 5. XPS spectrum of C1s for GOM-0.04 (a), rGOM-0.04 after 30 min UV (b), rGOM-0.04 after 60 min UV (c), GOM-0.06 (d), rGOM-0.06 after 30 min UV (e) and rGOM-0.06 after 60 min UV (f).

groups on the surface of the prepared membranes. Fig. 5 shows the C1s XPS spectrum of GOM and rGOM divided into four Gaussian peaks at 284.5, 286.4, 287.7, and 288.8 eV, corresponding to the typical signals of C-C/C=C, C-O, C=O, and O-C-O bonds, respectively [35]. As can be observed, before the reduction GOM mainly contained C-C/C=C bonds ascribable to aromatic rings and C-O bonds related to epoxy and alkoxy groups. After the UV-assisted reduction, the relative intensity of C-O bond peak gradually decreased while the intensity of C-C/C=C bonds peak increased, indicating substantial removal of the oxygen-containing groups from the surface of the membrane. The O1s XPS spectrum shown in Fig. 6 also confirmed the effect of the reduction in membrane composition. This spectrum was deconvoluted in four peaks with binding energies of 531.2, 532.5, 533.3 and 533.9 eV representing the O-C=O, C=O, C-OH and C-O-C bonds, respectively [36]. After UV-assisted reduction treatment, the intensity of the peaks decreased, mainly the peaks ascribable to carboxyl (C=O) and alkoxy (C-OH) groups, indicating reduction of GO. Wetting characteristics and hydrophilicity of the membranes can be expected to decrease with the partial or total removal of the oxygen-containing groups, particularly hydroxyl groups, affecting the permeability [18]. However, there is no consensus in literature about the effect on permeability of the removal of these groups, since contrary effects have been reported by Hou et al. [13] and Huang et al. [18]. C/O atomic ratios were quantified by XPS, and they are shown in Fig. 7. The carbon content in the membranes increased from 68.9 to 70.1 % to 77.2–78.8 % reduction with UV radiation for 60 min, while the oxygen content decreased from 28.9 to 29.8 % to 20.1–21.7 %. Accordingly, the C/O ratio increased from 2.3 to 2.4 in GOM to 3.6–3.9 in rGOM reduced for 60 min. Therefore, it can be

concluded that the UV-assisted reduction treatment significantly affected the distribution of functional groups in the GO membrane on Nylon support, producing substantial decrease in the oxygen-containing functional groups. The most drastic decrease took place during the first 30 min of reduction, affecting largely to the epoxy and alkoxy groups content, and indicating that longer reduction times lead only to a slightly increase in the reduction degree. After 60 min of UV treatment some oxygen-containing functional groups remained, which can act as spacers between graphene sheets and have a relevant role in water passage [18,19].

Regarding the effect of GO load in the membrane, no significant differences were observed in the chemical composition and distribution of the functional groups after UV-treatment. This observation indicates similar effect of UV-assisted reduction across the membrane depth that can be probed with XPS.

The morphology of the surface and cross-section of GOM-0.04 and GOM-0.06 membranes were analysed by SEM. A complete set of images is provided in supporting information, Fig. S1 and S2. As can be observed in Fig. 8 (a) and (c), the smoothness of the surface of the membranes increased with GO load. This change in texture can be related to the higher filtration time for the preparation of GOM-0.06 (1.5 h vs 1 h), enabling settling and staking of the GO sheets at the uppermost layers of the membrane. A thickness value around 80 nm was estimated for the membranes prepared using 0.04 mg cm⁻² of GO, which increased to around 104 nm for membranes prepared using 0.06 mg cm⁻². In the literature, some authors have also reported that a higher loading amount of GO leads to a higher membrane thickness [18,37], although the increase in thickness is not lineal due to differences in settling of GO sheets

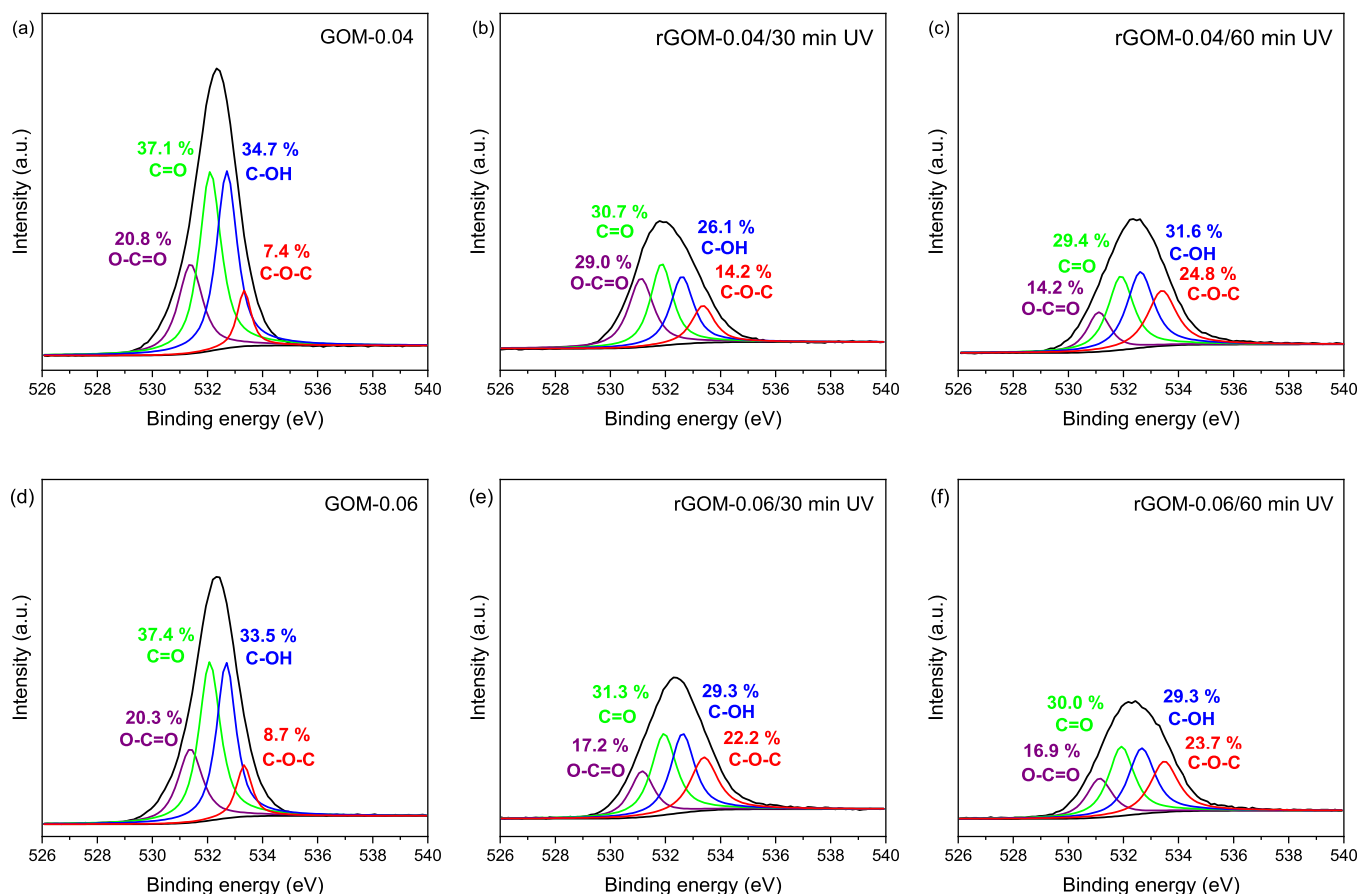


Fig. 6. XPS spectrum of O1s for GOM-0.04 (a), rGOM-0.04 after 30 min UV (b), rGOM-0.04 after 60 min UV (c), GOM-0.06 (d), rGOM-0.06 after 30 min UV (e) and rGOM-0.06 after 60 min UV (f).

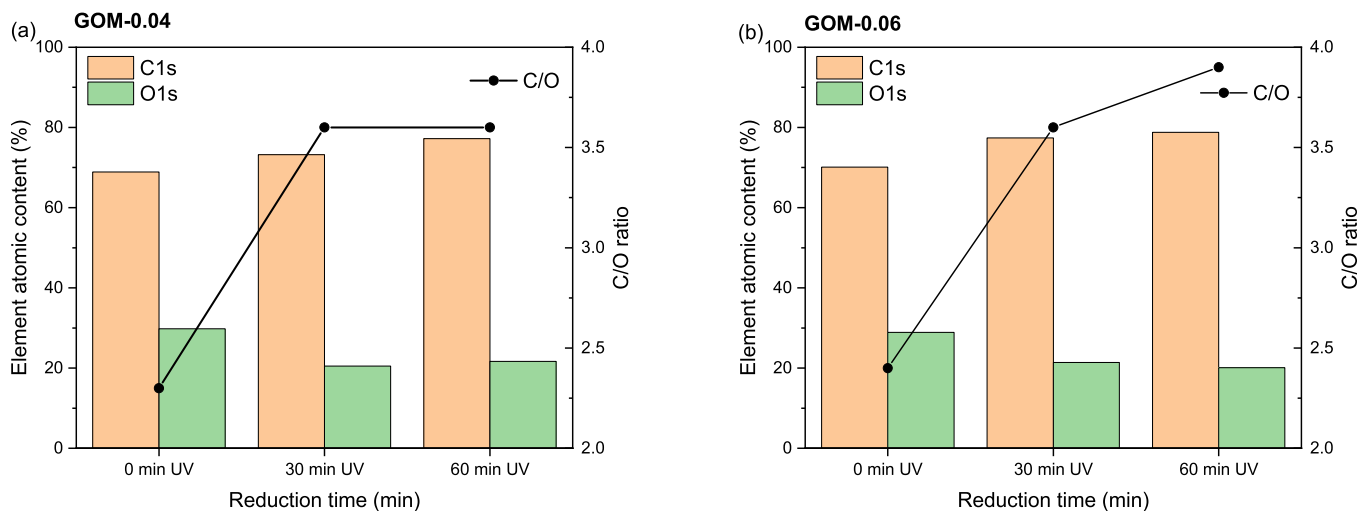


Fig. 7. Chemical composition obtained from XPS analysis of GO membranes on Nylon support.

during filtration.

The prepared membranes were also characterized by XRD to assess changes in interlayer spacing. Fig. 9 shows the XRD of GOM-0.04, GOM-0.06 and rGOM-0.06. The major XRD peak of GOM-0.04 and GOM-0.06 were found at 10.92° (interlayer spacing of 8.09 \AA) and 11.06° (interlayer spacing of 7.99 \AA), respectively. The lower interlayer spacing exhibited by GOM-0.06 compared to GOM-0.04 can be attributed partially to different formation times of the membranes, with higher

contribution of compaction and settling for GOM-0.06 and higher staking of GO sheets [15]. The XRD peak membranes shifted to higher values with reduction. Thus rGOM-0.06 showed a peak at 11.96° after reduction for 30 and 60 min, corresponding to interlayer spacing of 7.39 \AA . A similar behaviour was observed by Amadei et al. [38].

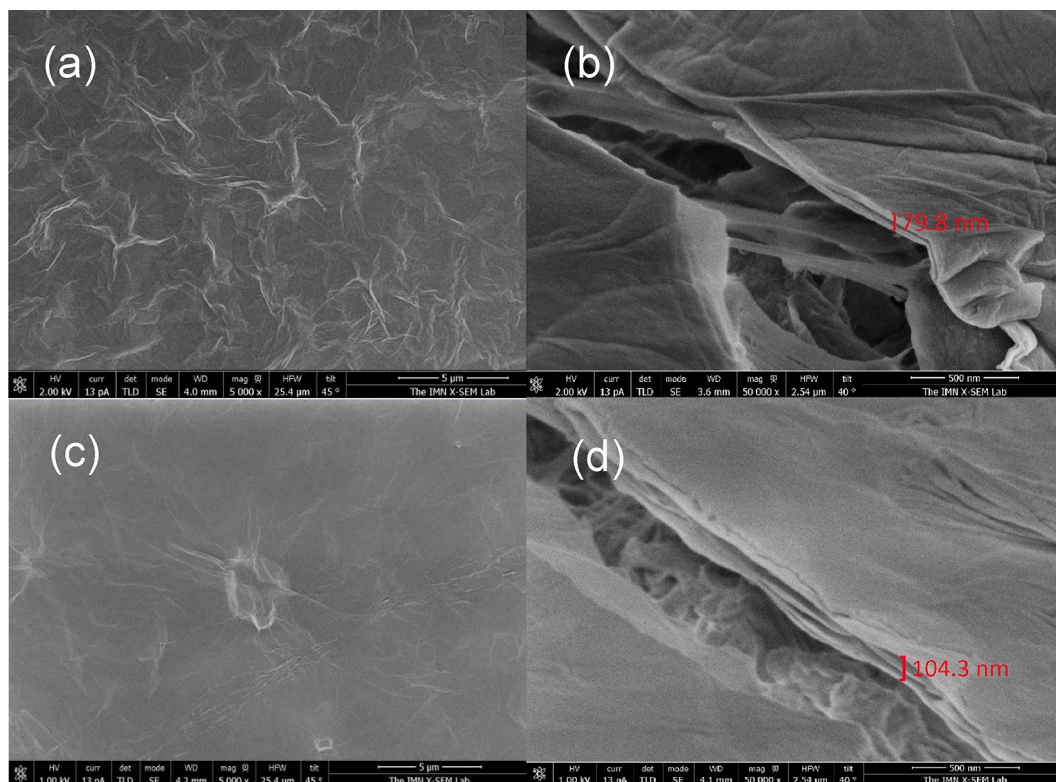


Fig. 8. SEM image of surface (a) GOM-0.04 (c) GOM-0.06, and cross-section of (b) GOM-0.04 and (d) GOM-0.06 membranes.

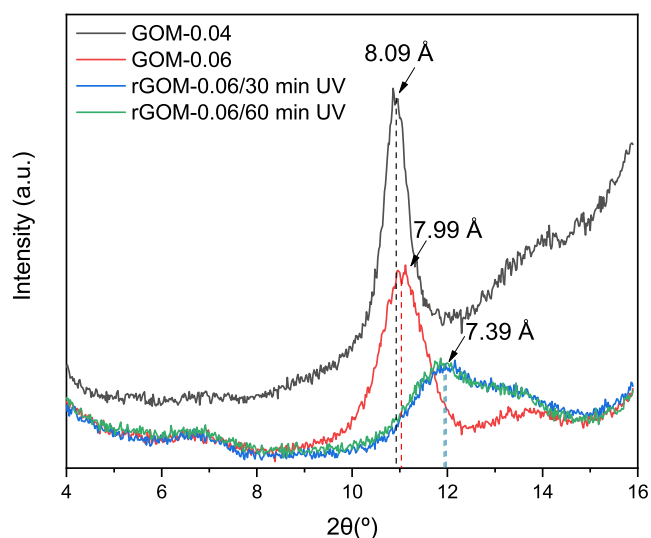


Fig. 9. XRD patterns and interlayer spacing of GOM-0.04, GOM-0.06 and rGOM-0.06 after 30 and 60 min of reduction.

3.2. Filtration performance of GO and rGO membranes on Nylon support

Pyridine, phenol, 2-naphthol and disperse blue 3 solutions were used as feed in the filtration experiments. All the membranes tested showed stability during the experiments, no separation from the support, delamination or surface damage were observed, both in the untreated and reduced membranes as it can be observed in supporting information (Figure S3). Stability is indicative of a good adhesion of the GO to the Nylon support even after the reduction and removal of oxygen functional groups.

Due to the microporous nature of the Nylon support, it did not retain

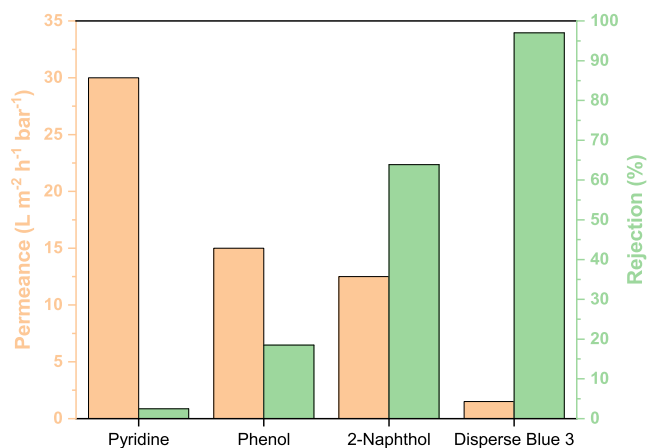


Fig. 10. Filtration performance of GOM-0.04 membrane for pyridine, phenol, 2-naphthol and disperse blue 3 solutions.

the solutes tested and showed a large permeability for water. Therefore, it was assumed that the support does not have direct influence in the rejection and permeability of GO membranes supported on Nylon. The results of permeance and rejection for GOM-0.04 membrane are shown in Fig. 10. The reproducibility of filtration tests was studied in selected experiments for non-irradiated and irradiated membranes, yielding values of $\pm 1.7 \text{ L m}^{-2} \text{ h}^{-1} \text{ bar}^{-1}$ for water permeance, $\pm 0.05\text{--}0.30 \text{ L m}^{-2} \text{ h}^{-1} \text{ bar}^{-1}$ for solute solution permeance, and $\pm 2\text{--}9 \%$ for solute rejection. Rejection increased with increasing molecular size of the organic compound used as probe. A molecular weight cut-off (MWCO) lower than 300 Da can be attributed to the membrane according to rejection value above 90 % observed for disperse blue 3. Relevant differences in rejection were observed for 2-naphthol (64 %) and phenol (19 %) despite relatively low differences in molecular weight. These results show the potential of GO for preparing membranes with low MWCOs.

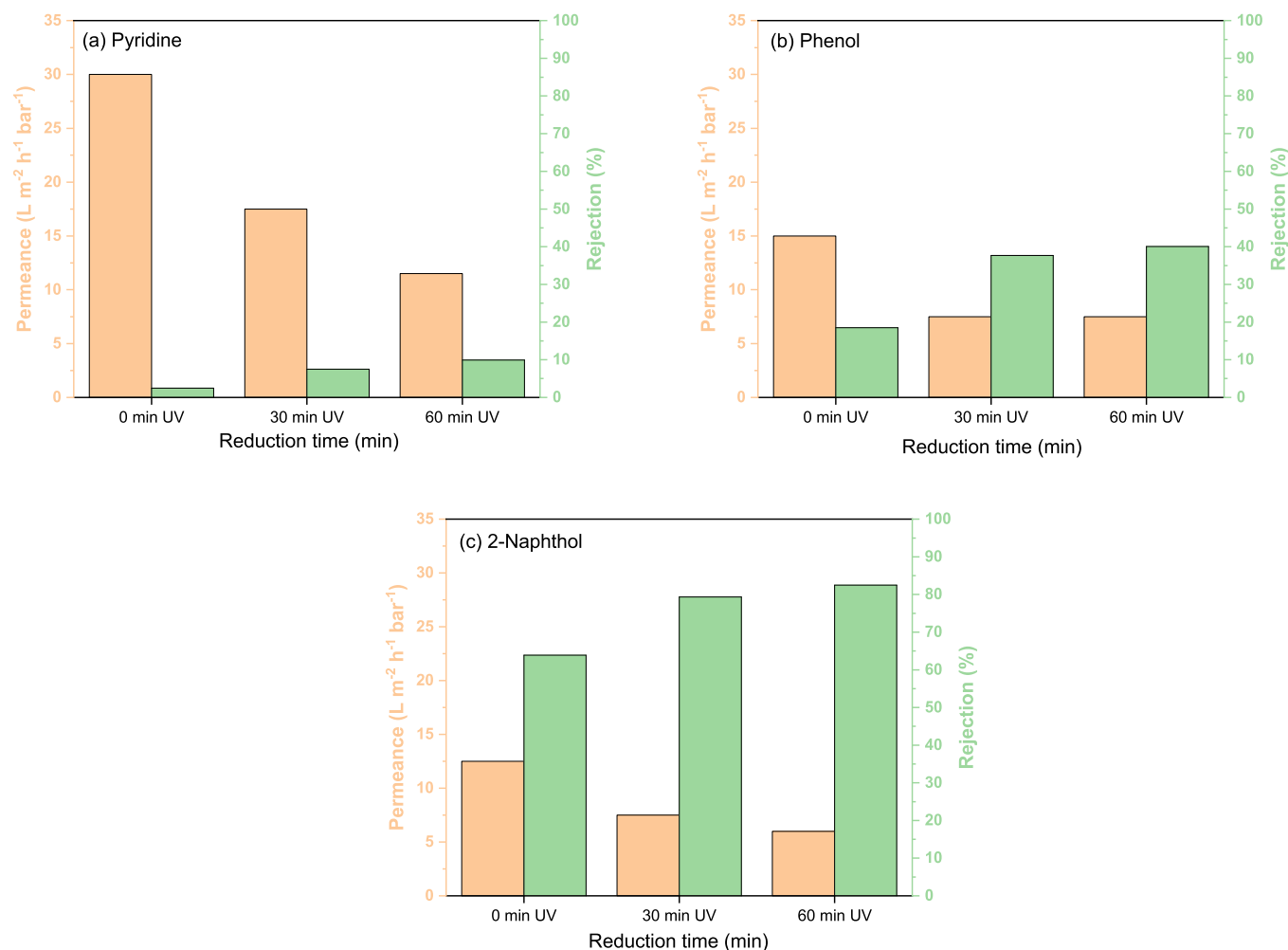


Fig. 11. Permeation performance of GOM-0.04, rGOM-0.04 after 30 min UV and rGOM-0.04 after 60 min UV in filtration tests with pyridine (a), phenol (b) and 2-naphthol (c) solution.

Permeance decreased with increasing molecular size, which can be related to polarization of the membrane or blockage of pores by rejected solute molecules.

The filtration performance of rGOM-0.04 for pyridine, phenol and 2-naphthol solutions is shown in Fig. 11. It can be seen that the rejection observed for GOM-0.04 increased with UV reduction and that permeance decreased. In the case of phenol and 2-naphthol a significant change in both rejection and permeance was obtained after the 30 min UV reduction treatment, whereas additional but minor changes were obtained by UV reduction for 60 min. Therefore, the reduction and removal of oxygen surface groups results in staking of GO sheets, lower interlayer space and narrower pores, enabling higher rejection of solutes [38]. A rejection of 83 % was obtained for 2-naphthol showing that UV-reduction can be used to tune the MWCO of the membrane, achieving a remarkably low value close to 150 Da. Commercial nanofiltration typically have MWCOs for dissolved organic solutes of 200–1000 Da [39]. Thus the irradiation of the GO membranes on Nylon support makes possible to achieve the low MWCO of nanofiltration with moderate loss of permeance. The decrease in the permeance can also be related to narrower pores for permeation, although a lower hydrophilicity of the membranes reduced by UV radiation can be expected from the removal of oxygen surface groups [38].

The results for pyridine show gradual increase of rejection with UV-assisted reduction time, increasing from 2.5 % for GOM-0.04 to 7.5 and 9.9 % after 30 and 60 min, respectively. Therefore, although increasing UV-assisted reduction time from 30 to 60 min led to minor effects on

surface oxygen groups and interlayer space, fine tuning of the porosity of the membrane and better control of the rejection of low molecular size solutes was achieved. Enhanced reduction can be expected to enable even higher rejection for this range of solute size. In the case of the filtration of pyridine solution permeance also decreased gradually with UV reduction time.

Fig. 12 shows the performance in the filtration of pyridine, phenol and 2-naphthol solutions of GOM-0.04 and GOM-0.06, and also of rGOM-0.04 and rGOM-0.06 after reduction for 30 and 60 min. For all the feed solutions tested, when GO load increased from 0.04 to 0.06 mg cm⁻², permeance decreased and rejection increased. The higher rejection can be related to the higher thickness of the GOM-0.06, but also to compaction and settling during the preparation of the membrane by filtration of GO solution. Thus, Abraham et al. [40] reported that the water permeance decreased monotonically with decreasing the interlayer spacing of GO in membranes. Likewise, as previously described from SEM images, the membranes prepared with a higher load of GO exhibited smoother surface. In the literature, wrinkles on the surface of the membranes have been associated to channels for permeation of water and solute molecules [13].

The change in filtration performance of GOM-0.04 and GOM-0.06 membrane due to UV-assisted reduction followed similar trends, although in general higher rejection and lower permeance was observed for the membranes with higher GO load. Thus, differences in filtration behaviour due to UV reduction were much higher than changes due to GO load. Therefore, UV-reduction shows a high potential for tuning the

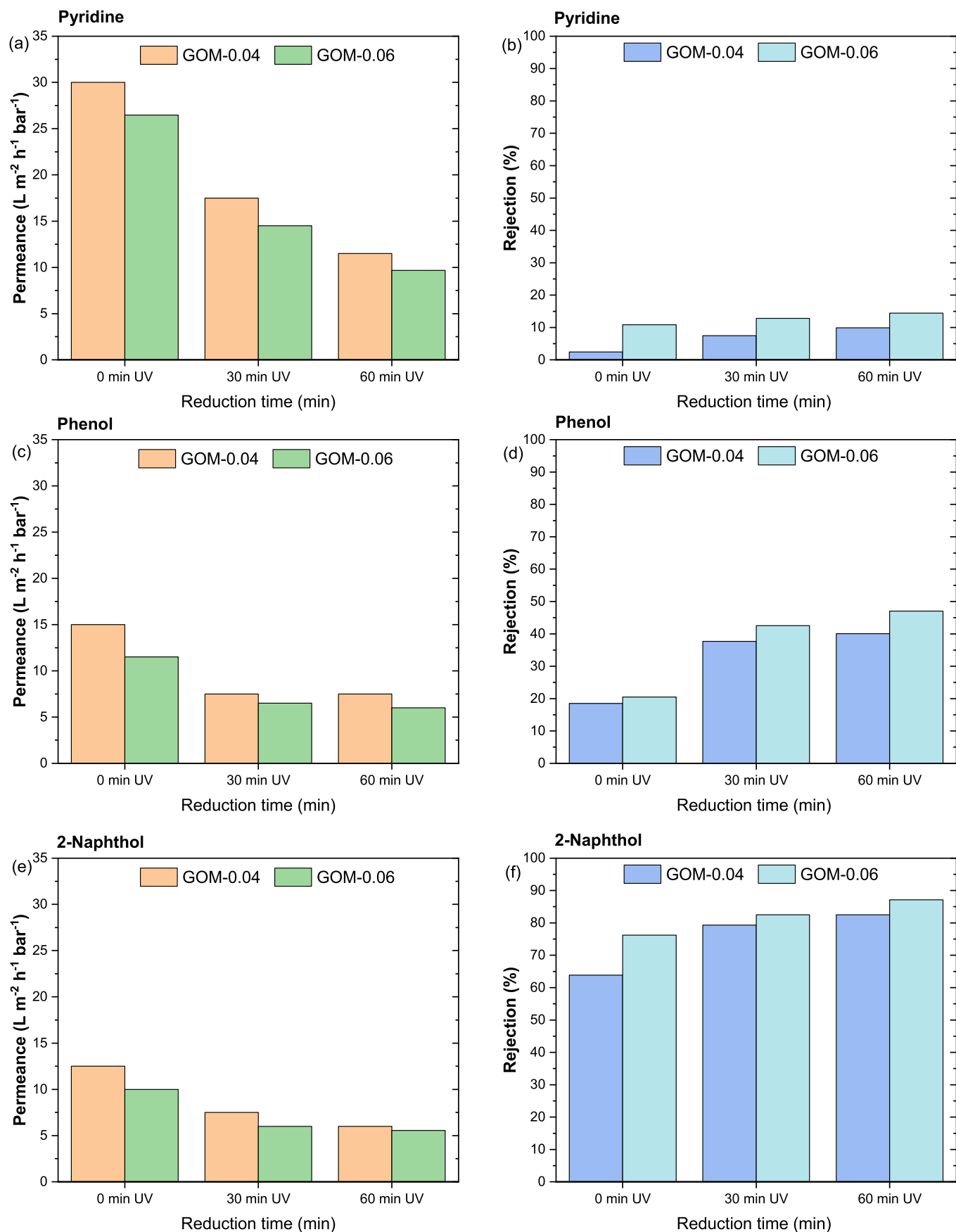


Fig. 12. Permeation performance of GOM-0.04, GOM-0.06, rGOM-0.04 and rGOM-0.06 after 30 min and 60 min UV tested with pyridine (a and b), phenol (c and d) and 2-naphthol (e and f).

properties of GO membranes on Nylon support and achieving high rejection of small molecules in the range of the molecular size of micropollutant typically occurring in polluted water and reclaimed water. Further work is needed in the improvement of permeance, which may be largely affected by decrease in hydrophilicity.

4. Conclusion

Graphene oxide membranes on Nylon support (GOM) were prepared by using different GO load and UV-assisted reduction time, and used in the filtration of solutes representative of low molecular size pollutants. The permeance value decreased and the rejection increased with GO load due to higher thickness and lower interlayer spacing, the latter attributed to compaction and settling during the preparation of this membrane. UV-assisted reduction treatment resulted in the removal of oxygen surface groups, staking of GO sheets, and a decrease in interlayer space and pore size, which led to higher rejection of tested solutes. In general, higher rejection and lower permeance were obtained for the membranes with a higher GO load regardless the reduction time used. Differences in the filtration behaviour due to the UV reduction was higher than the differences due to the GO load. UV-assisted reduction treatment shows a high potential for tuning of GO membranes on Nylon support properties and performance.

CRediT authorship contribution statement

M. Fernández-Márquez: Data curation, Investigation, Methodology. **R. Pla:** Data curation, Investigation, Writing – original draft. **A.S. Oliveira:** Data curation, Investigation, Writing – original draft. **J.A. Baeza:** Validation, Writing – review & editing. **L. Calvo:** Conceptualization, Supervision, Writing – review & editing, Funding acquisition. **N. Alonso-Morales:** Conceptualization, Supervision, Writing – review & editing, Funding acquisition. **M.A. Gilarranz:** Writing – review & editing, Funding acquisition.

Declaration of Competing Interest

The authors declare that they have no known competing financial interests or personal relationships that could have appeared to influence the work reported in this paper.

Data availability

No data was used for the research described in the article.

Acknowledgements

The authors greatly appreciate financial support from Spanish AEI through the projects RTI2018-098431-B-I00 and PID2021-122248OB-I00, and the Comunidad de Madrid for Manuel Fernández-Márquez (PEJ-2018-AI/IND-11505; PEJ-2018PR-AI/IND-20881) and Raul Pla (PEJ-2020-AI/IND-18302) financial support.

Appendix A. Supplementary data

Supplementary data to this article can be found online at <https://doi.org/10.1016/j.cej.2022.137807>.

References

- [1] A. Boretti, L. Rosa, Reassessing the projections of the world water development report, *Npj Clean Water*. 2 (2019), <https://doi.org/10.1038/s41545-019-0039-9>.
- [2] P. Mukheibir, Water access, water scarcity, and climate change, *Environ. Manage.* 45 (2010) 1027–1039, <https://doi.org/10.1007/s00267-010-9474-6>.
- [3] R. Rashid, I. Shafiq, P. Akhter, M.J. Iqbal, M. Hussain, A state-of-the-art review on wastewater treatment techniques: the effectiveness of adsorption method, *Environ.*

- Sci. Pollut. Res.* 28 (2021) 9050–9066, <https://doi.org/10.1007/s11356-021-12395-x>.
- [4] M.B. Ahmed, J.L. Zhou, H.H. Ngo, W. Guo, N.S. Thomaidis, J. Xu, Progress in the biological and chemical treatment technologies for emerging contaminant removal from wastewater: A critical review, *J. Hazard. Mater.* 323 (2017) 274–298, <https://doi.org/10.1016/j.jhazmat.2016.04.045>.
- [5] P.R. Rout, T.C. Zhang, P. Bhunia, R.Y. Surampalli, Treatment technologies for emerging contaminants in wastewater treatment plants: A review, *Sci. Total Environ.* 753 (2021), 141990, <https://doi.org/10.1016/j.scitotenv.2020.141990>.
- [6] J.F.J.R. Pesqueira, M.F.R. Pereira, A.M.T. Silva, Environmental impact assessment of advanced urban wastewater treatment technologies for the removal of priority substances and contaminants of emerging concern: A review, *J. Clean. Prod.* 261 (2020), 121078, <https://doi.org/10.1016/j.jclepro.2020.121078>.
- [7] A. Alkhousaam, H. Qiblawey, Functional GO-based membranes for water treatment and desalination: Fabrication methods, performance and advantages, A review, *Chemosphere*. 274 (2021), 129853, <https://doi.org/10.1016/j.chemosphere.2021.129853>.
- [8] E.O. Ezugbe, S. Rathilal, Membrane technologies in wastewater treatment: A review, *Membranes (Basel)*. 10 (2020) 89, <https://doi.org/10.3390/membranes10050089>.
- [9] J. Ma, D. Ping, X. Dong, Recent developments of graphene oxide-based membranes: A Review, *Membranes (Basel)*. 7 (2017) 52, <https://doi.org/10.3390/membranes7030052>.
- [10] P. Bhol, S. Yadav, A. Altaee, M. Saxena, P.K. Misra, A.K. Samal, Graphene-based membranes for water and wastewater treatment: A Review, *ACS Appl. Nano Mater.* 4 (2021) 3274–3293, <https://doi.org/10.1021/acsanm.0c03439>.
- [11] E.F.D. Januário, T.B. Vidovich, N.d.C.L. Beluci, R.M. Paixão, L.H.B.R.d. Silva, N. C. Homem, R. Bergamasco, A.M.S. Vieira, Advanced graphene oxide-based membranes as a potential alternative for dyes removal: A review, *Sci. Total Environ.* 789 (2021) 147957.
- [12] S. El Meragawi, A. Akbari, S. Hernandez, M.S. Mirshekarloo, D. Bhattacharyya, A. Tanksale, M. Majumder, Enhanced permselective separation of per-fluorooctanoic acid in graphene oxide membranes by a simple PEI modification, *J. Mater. Chem. A*. 8 (2020) 24800–24811, <https://doi.org/10.1039/D0TA06523D>.
- [13] J. Hou, C. Bao, S. Qu, X. Hu, S. Nair, Y. Chen, Graphene oxide membranes for ion separation: Detailed studies on the effects of fabricating conditions, *Appl. Surf. Sci.* 459 (2018) 185–193, <https://doi.org/10.1016/j.apsusc.2018.07.207>.
- [14] Y. Wei, X. Gao, X. Wang, B. He, C. Gao, The influence of nanosheets' size on pressure assisted self-assembly graphene oxide nanofiltration membrane, *Desalination Water Treat.* 201 (2020) 43–54, <https://doi.org/10.5004/dwt.2020.25813>.
- [15] W.L. Xu, C. Fang, F. Zhou, Z. Song, Q. Liu, R. Qiao, M. Yu, Self-assembly: A facile way of forming ultrathin, high-performance graphene oxide membranes for water purification, *Nano Lett.* 17 (2017) 2928–2933, <https://doi.org/10.1021/acs.nanolett.7b00148>.
- [16] K. Yang, L. Huang, Y. Wang, Y. Du, Z. Zhang, Y. Wang, M.J. Kipper, L.A. Belfiore, J. Tang, Graphene oxide nanofiltration membranes containing silver nanoparticles: Tuning separation efficiency via nanoparticle size, *Nanomaterials*. 10 (2020) 454, <https://doi.org/10.3390/nano10030454>.
- [17] Y. Qian, X. Zhang, C. Liu, C. Zhou, A. Huang, Tuning interlayer spacing of graphene oxide membranes with enhanced desalination performance, *Desalination*. 460 (2019) 56–63, <https://doi.org/10.1016/j.desal.2019.03.009>.
- [18] H.-H. Huang, R.K. Joshi, K.K.H. De Silva, R. Badam, M. Yoshimura, Fabrication of reduced graphene oxide membranes for water desalination, *J. Memb. Sci.* 572 (2019) 12–19, <https://doi.org/10.1016/j.memsci.2018.10.085>.
- [19] Y. Gao, Y. He, S. Yan, H. Yu, J. Ma, R. Hou, Y. Fan, X. Yin, Controlled reduction and fabrication of graphene oxide membrane for improved permeance and water purification performance, *J. Mater. Sci.* 55 (2020) 15130–15139, <https://doi.org/10.1007/s10853-020-05073-9>.
- [20] W.D. Yang, Y.R. Li, Y.C. Lee, Synthesis of r-GO/TiO₂ composites via the UV-assisted photocatalytic reduction of graphene oxide, *Appl. Surf. Sci.* 380 (2016) 249–256, <https://doi.org/10.1016/j.apsusc.2016.01.118>.
- [21] R. Yi, X. Xia, R. Yang, R. Yu, F. Dai, J. Chen, W. Liu, M. Wu, J. Xu, L. Chen, Selective reduction of epoxy groups in graphene oxide membrane for ultrahigh water permeation, *Carbon N. Y.* 172 (2021) 228–235, <https://doi.org/10.1016/j.carbon.2020.09.076>.
- [22] Y.L. Zhang, L. Guo, H. Xia, Q.D. Chen, J. Feng, H.B. Sun, Photoreduction of Graphene Oxides: Methods, Properties, and Applications, *Adv. Opt. Mater.* 2 (2014) 10–28, <https://doi.org/10.1002/adom.201300317>.
- [23] H. Yu, Y. He, G. Xiao, Y. Fan, J. Ma, Y. Gao, R. Hou, J. Chen, Weak-reduction graphene oxide membrane for improving water purification performance, *J. Mater. Sci. Technol.* 39 (2020) 106–112, <https://doi.org/10.1016/j.jmst.2019.08.024>.
- [24] V.G. Plotnikov, V.A. Smirnov, M.V. Alfimov, Y.M. Shul'ga, The graphite oxide photoreduction mechanism, *High Energy Chem.* 45 (2011) 411–415, <https://doi.org/10.1134/S0018143911050158>.
- [25] V.A. Smirnov, N.N. Denisov, V.G. Plotnikov, M.V. Alfimov, Photochemical processes in graphene oxide films, *High Energy Chem.* 50 (2016) 51–59, <https://doi.org/10.1134/S0018143916010070>.
- [26] O. Kwon, Y. Choi, E. Choi, M. Kim, Y.C. Woo, D.W. Kim, Fabrication techniques for graphene oxide-based molecular separation membranes: Towards industrial application, *Nanomaterials*. 11 (2021) 1–15, <https://doi.org/10.3390/nano11030757>.
- [27] J. Wang, X. Gao, H. Yu, Q. Wang, Z. Ma, Z. Li, Y. Zhang, C. Gao, Accessing of graphene oxide (GO) nanofiltration membranes for microbial and fouling

- resistance, *Sep. Purif. Technol.* 215 (2019) 91–101, <https://doi.org/10.1016/J.SEPPUR.2019.01.018>.
- [28] Z. Liu, Z. Ma, B. Qian, A.Y.H. Chan, X. Wang, Y. Liu, J.H. Xin, A Facile and Scalable Method of Fabrication of Large-Area Ultrathin Graphene Oxide Nanofiltration Membrane, *ACS Nano*. 15 (2021) 15294–15305, <https://doi.org/10.1021/acsnano.1c06155>.
- [29] D.-G. Thomas, E. Kavak, N. Hashemi, R. Montazami, N. Hashemi, Synthesis of Graphene Nanosheets through Spontaneous Sodiation Process, *C - J. Carbon Res.* 4 (2018) 42, <https://doi.org/10.3390/c4030042>.
- [30] M. Zhang, Y. Mao, G. Liu, G. Liu, Y. Fan, W. Jin, Molecular Bridges Stabilize Graphene Oxide Membranes in Water, *Angew. Chemie - Int. Ed.* 59 (2020) 1689–1695, <https://doi.org/10.1002/anie.201913010>.
- [31] X. Fan, C. Cai, J. Gao, X. Han, J. Li, Hydrothermal reduced graphene oxide membranes for dyes removing, *Sep. Purif. Technol.* 241 (2020), 116730, <https://doi.org/10.1016/J.SEPPUR.2020.116730>.
- [32] N.K.E.M. Khor, T. Salmiati, Z.Y. Hadibarata, A combination of waste biomass activated carbon and nylon nanofiber for removal of triclosan from aqueous solutions, *J. Environ. Treat. Tech.* 8 (2020) 1036–1045, [https://doi.org/10.47277/jett-8\(3\)1](https://doi.org/10.47277/jett-8(3)1).
- [33] H. Wu, J. Fan, E. Liu, X. Hu, Y. Ma, X. Fan, Y. Li, C. Tang, Facile hydrothermal synthesis of TiO₂ nanospindles-reduced graphene oxide composite with a enhanced photocatalytic activity, *J. Alloys Compd.* 623 (2015) 298–303, <https://doi.org/10.1016/J.JALLCOM.2014.10.153>.
- [34] C. Nethravathi, M. Rajamathi, Chemically modified graphene sheets produced by the solvothermal reduction of colloidal dispersions of graphite oxide, *Carbon N. Y.* 46 (2008) 1994–1998, <https://doi.org/10.1016/J.CARBON.2008.08.013>.
- [35] L. Zhang, F. Dai, R. Yi, Z. He, Z. Wang, J. Chen, W. Liu, J. Xu, L. Chen, Effect of physical and chemical structures of graphene oxide on water permeation in graphene oxide membranes, *Appl. Surf. Sci.* 520 (2020), 146308, <https://doi.org/10.1016/j.apsusc.2020.146308>.
- [36] R. Al-Gaashani, A. Najjar, Y. Zakaria, S. Mansour, M.A. Atieh, XPS and structural studies of high quality graphene oxide and reduced graphene oxide prepared by different chemical oxidation methods, *Ceram. Int.* 45 (2019) 14439–14448, <https://doi.org/10.1016/J.CERAMINT.2019.04.165>.
- [37] Y. Zhang, L.J. Huang, Y.Y.X. Wang, J.G. Tang, Y.Y.X. Wang, M.M. Cheng, Y.C. Du, K. Yang, M.J. Kipper, M. Hedayati, The preparation and study of ethylene glycol-modified graphene oxide membranes for water purification, *Polymers (Basel)*. 11 (2019) 1–12, <https://doi.org/10.3390/polym11020188>.
- [38] C.A. Amadei, A. Montessori, J.P. Kadow, S. Succi, C.D. Vecitis, Role of oxygen functionalities in graphene oxide architectural laminate subnanometer spacing and water transport, *Environ. Sci. Technol.* 51 (2017) 4280–4288, <https://doi.org/10.1021/acs.est.6b05711>.
- [39] I. Koyuncu, R. Sengur, T. Turken, S. Guclu, M.E. Pasaoglu, Advances in water treatment by microfiltration, ultrafiltration, and nanofiltration, *Adv. Membr. Technol. Water Treat. Mater. Process. Appl.* (2015) 83–128, <https://doi.org/10.1016/B978-1-78242-121-4.00003-4>.
- [40] J. Abraham, K.S. Vasu, C.D. Williams, K. Gopinadhan, Y. Su, C.T. Cherian, J. Dix, E. Prestat, S.J. Haigh, I.V. Grigorieva, P. Carbone, A.K. Geim, R.R. Nair, Tunable sieving of ions using graphene oxide membranes, *Nat. Nanotechnol.* 12 (2017) 546–550, <https://doi.org/10.1038/nnano.2017.21>.